JOURNAL OF VIROLOGY, Oct. 2004, p. 10636–10649 Vol. 78, No. 19
0022-538X/04/$08.00+0 DOI: 10.1128/JVI.78.19.10636–10649.2004

Activation of TBK1 and IKKε Kinases by Vesicular Stomatitis Virus Infection and the Role of Viral Ribonucleoprotein in the Development of Interferon Antiviral Immunity

Benjamin R. tenOever,[1,2]† Sonia Sharma,[1,3]† Wen Zou,[1,2] Qiang Sun,[1,2] Nathalie Grandvaux,[1,2] Ilkka Julkunen,[4] Hiroaki Hemmi,[5] M. Yamamoto,[5] Shizuo Akira,[5] Wen-Chen Yeh,[6] Rongtuan Lin,[1,2] and John Hiscott[1,2,3]*

Terry Fox Molecular Oncology Group, Lady Davis Institute for Medical Research,[1] and Departments of Microbiology and Immunobiology[3] and Medicine,[2] McGill University, Montreal, Quebec, and Advanced Medical Discovery Institute, University Health Network and the Department of Medical Biophysics, University of Toronto, Toronto, Ontario,[6] Canada; Department of Host Defense, Research Institute for Microbial Diseases, Osaka University, Yamada-oka, Suita, Osaka, Japan[5]; and National Public Health Institute, Helsinki, Finland[4]

Received 1 April 2004/Accepted 17 May 2004

Mounting an immune response to a viral pathogen involves the initial recognition of viral antigens through Toll-like receptor-dependent and -independent pathways and the subsequent triggering of signal transduction cascades. Among the many cellular kinases stimulated in response to virus infection, the noncanonical IKK-related kinases TBK1 and IKKε have been shown to phosphorylate and activate interferon regulatory factor 3 (IRF-3) and IRF-7, leading to the production of alpha/beta interferons and the development of a cellular antiviral state. In the present study, we examine the activation of TBK1 and IKKε kinases by vesicular stomatitis virus (VSV) infection in human lung epithelial A549 cells. We demonstrate that replication-competent VSV is required to induce activation of the IKK-related kinases and provide evidence that ribonucleoprotein (RNP) complex of VSV generated intracellularly during virus replication can activate TBK1 and IKKε activity. In TBK1-deficient cells, IRF-3 and IRF-7 activation is significantly reduced, although transcriptional upregulation of IKKε following treatment with VSV, double-stranded RNA, or RNP partially compensates for the loss of TBK1. Biochemical analyses with purified TBK1 and IKKε kinases in vitro demonstrate that the two kinases exhibit similar specificities with respect to IRF-3 and IRF-7 substrates and both kinases target serine residues that are important for full transcriptional activation of IRF-3 and IRF-7. These data suggest that intracellular RNP formation contributes to the early recognition of VSV infection, activates the catalytic activity of TBK1, and induces transcriptional upregulation of IKKε in epithelial cells. Induction of IKKε potentially functions as a component of the amplification mechanism involved in the establishment of the antiviral state.

The immediate cellular response to virus infection represents an early stage at which active immunity can be mounted against viral pathogens. In response to the rapid replication of viruses, the early cellular antiviral defense limits virus replication to provide time for the development of the adaptive immune response, necessary for clearance of the viral pathogen (13, 45). Viral proteins and by-products of the virus life cycle are recognized by evolutionarily conserved Toll-like receptors (TLRs) that trigger activation of multiple signaling cascades (38). TLRs recognize biochemically conserved molecules that are exclusive to foreign pathogens. Collectively termed pathogen-associated molecular patterns, gram-negative bacterial lipopolysaccharide (LPS), bacterial flagellin, and viral double-stranded RNA (dsRNA) represent some of the ligands that initiate innate immune responses through TLR signaling (31, 39, 53).

Included in the early signaling events initiated by virus infection are regulatory kinases such as p38/JNK, the classical IKK complex IKKα/IKKβ/IKKγ, and the noncanonical IKK-related complex IKKε/TBK1, which respectively activate the AP-1, NF-κB, and interferon (IFN) regulatory factor (IRF) transcription factors (4, 8, 18, 49). These transcription factors coordinate the production of cytokines, which in turn communicate the presence of the viral pathogen to neighboring cells through the production of beta IFN (IFN-β) and IFN-α1 and recruit the innate immune machinery through chemokines such as RANTES, IP-10, MIP1α, and MIP1β (40, 45). Although AP-1 and NF-κB activation occurs in response to an array of cellular stimuli, IRF-3 and IRF-7 activation appears to represent a more restricted response against pathogen infection (46). The absence of IRF-3 and IRF-7 in murine knockout models results in low IFN-β and RANTES production in response to virus infection (42), thus supporting a pivotal role for IRF-3–IRF-7 activation in the development of the cellular antiviral response.

IRF-3 is a phosphoprotein that is constitutively expressed in all cell types as two latent, predominantly cytoplasmic forms (I and II), with an amino-terminal tryptophan repeat-containing DNA binding domain and a carboxyl-terminal IRF association

* Corresponding author. Mailing address: Lady Davis Institute for Medical Research, McGill University, 3755 Cote Ste. Catherine, Montreal, Quebec, Canada H3T 1E2. Phone: (514) 340-8222, ext. 5265. Fax: (514) 340-7576. E-mail: john.hiscott@mcgill.ca.

† B.R.T. and S.S. contributed equally to the work.

domain (IAD) and transactivation domain. The transcriptional activity of IRF-3 is controlled by C-terminal phosphorylation events on serines 385 and 386 (32, 58) and 396, 398, 402, and 405 as well as threonine 404 (24, 47). The exact residues targeted by virus infection remain controversial (32, 47); however, it is clear that phosphorylation within the serine/threonine C-terminal cluster induces a conformation change within IRF-3 that allows dimerization, nuclear localization, and association with its coactivator CBP/p300 (24, 26, 58). Since IRF-3 constitutively shuttles in and out of the nucleus, phosphorylation-dependent association with CBP/p300 is believed to retain IRF-3 in the nucleus. Once bound to its coactivator, IRF-3 binds consensus sites termed IFN-stimulated response elements (ISREs) to induce the transcriptional activation of target genes that include ISG56, RANTES, and IFN-β (12, 23, 43). Sustained activation of IRF-3 has also been found to induce cellular apoptosis (15, 55).

The IKK-related kinases TBK1 and IKKε function as essential components of the virus-activated kinase complex that phosphorylate and activate IRF-3, as well as the closely related IRF-7 (49). Intense study of innate immune signaling through TLRs has placed the TBK1 and IKKε upstream of IRF-3 and IRF-7 activation and IFN-α/β production (8, 30, 53). TBK1 and IKKε are activated downstream of dsRNA through TLR3 signaling (8), as a component of a MyD88-independent pathway regulated by the TLR-associated TIR adaptor molecule TRIF/TICAM-1 (16, 34, 44, 56, 57). IFN-α/β production in response to LPS signaling through TLR4 also requires TBK1 and IKKε kinase activity and acts through a MyD88-independent pathway involving TRIF together with a distinct TIR domain adaptor molecule, TRAM/TICAM-2 (9, 34). The TRIF adaptor directly interacts with TBK1 (9, 44), an event that requires intact TBK1 kinase activity and results in the posttranslational modification of TRIF by phosphorylation (44). Interestingly, the domain of TRIF that associates with TBK1 is in high proximity to the TRAF6 interaction domain, a region of TRIF required to activate the classical IKK–NF-κB signaling downstream of dsRNA-TLR3 engagement (44). Based on these results, MyD88-independent signaling appears to bifurcate into two distinct pathways downstream of the TRIF/TICAM-1 adaptor: a TRAF6-dependent cascade that leads to classical IKK–NF-κB activation and transcriptional upregulation of proinflammatory genes such as interleukin-6 (IL-6), IL-1β and tumor necrosis factor alpha and a TRAF6-independent IKK-related cascade that leads directly into IRF activation and production of TLR3-specific genes such as those for IFN-α/β, RANTES, and IP-10 cytokines (7, 8, 44, 56).

In the present study we sought to identify the viral determinants responsible for TBK1 or IKKε activation leading to the phosphorylation of IRF-3 in response to vesicular stomatitis virus (VSV) infection. We demonstrate in a human lung epithelial cell model that VSV-induced TBK1 activation requires replication-competent virus and production of viral ribonucleoprotein (RNP) complex. Virus and RNP activation appear to act independently of the TLR3-TRIF pathway, based on experiments in knockout murine embryonic fibroblasts (MEFs). These data suggest that the host recognition of VSV infection is triggered by intracellular RNP formation, which activates the catalytic activity of TBK1 and the transcriptional upregulation of IKKε.

MATERIALS AND METHODS

Plasmid construction and mutagenesis. Plasmids encoding wild-type (wt) IRF-7; IRF-7 A477/479, D471/472, D477/479, D483/487, and D475-479; IKKε; TBK1; glutathione *S*-transferase–IRF-3 (amino acids 380 to 427) [GST-IRF-3(aa380-427)]; GST-IRF-3-5A(aa380-427); GST-IRF-7(aa468-503); RANTES/pGL3; IFNB/pGL3; IFNA14/pGL3; and pRLTK were described previously (22, 49). The IRF-7 point mutants including A471/472, A475/476, A479, A483, A487, A483/487, D475/476, D477, and D479 were generated by overlap PCR mutagenesis with Vent DNA polymerase, and mutations were confirmed by sequencing. GST-IRF-3(aa380-427) peptide mutants including 3A, 7A, 396/398A, 398/402A, and 385/386A and GST-IRF-7(aa468-503) peptide mutants including 7A, 471/472A, 475/476A, 477/479A, 483/487A, 479A, 483A, and 487A were constructed using in vitro site-directed mutagenesis to introduce specific serine- or threonine-to-alanine mutations.

Cell culture, transfections, and reagents. BHK-21 T7 cells (a gift from K. Conzelmann, Federal Research Centre, Munich, Germany) and Vero African green monkey kidney cells (ATCC CCL-81) were maintained in Dulbecco's modified Eagle's medium supplemented with 10% fetal bovine serum (FBS). A549 human lung carcinoma cells (ATCC CCL-185) were maintained in F-12K medium supplemented with 10% FBS. All transfections were performed on 95% confluent tissue culture dishes with Lipofectamine 2000 (Invitrogen) as recommended by the manufacturer, with the exception of data for reverse transcriptase PCR (RT-PCR) in which Lipofectamine (Invitrogen) was used. Ribavirin (Sigma) was resuspended in double-distilled water (ddH_2O) and used at a concentration of 500 μg/ml. Cycloheximide (Sigma) was suspended in dimethyl sulfoxide (DMSO) and used at a concentration of 200 μg/ml. For both ribavirin and cycloheximide, A549 cells were pretreated half an hour prior to virus infection in addition to being present for the duration of the infection. dsRNA (Sigma) was heated to 50°C and allowed to cool to room temperature prior to transfection; VSV RNP was used directly from a large-scale isolation stock.

Viral infections. wt VSV (Indiana) was propagated in Vero cells and quantified by standard plaque assay. Virus infections were performed in the absence of serum for 1 h, after which growth medium was removed and replaced with fully supplemented growth medium. Plaque assays for viral quantification were performed in duplicate with log dilutions on 100% confluent Vero cells plated in six-well dishes. At 1 h after virus inoculation, medium was removed and replaced with 1% methylcellulose resuspended in complete growth medium. Three days postinfection, methylcellulose was removed and the cells were fixed with 4% formaldehyde for a minimum of 30 min at room temperature. Once fixed, cells were stained with 0.2% crystal violet (resuspended in 20% ethyl alcohol) and washed with water. Visible plaques were counted in duplicate and averaged to determine the working titer.

Immunoblot analysis. To investigate the phosphorylation state of IRF-3, whole-cell extracts (WCE) were subjected to sodium dodecyl sulfate-polyacrylamide gel electrophoresis (SDS-PAGE) on a 7.5% polyacrylamide gel. Following electrophoresis, proteins were transferred to Hybond-C transfer membrane (Amersham) in a buffer containing 30 mM Tris, 200 mM glycine, and 20% methanol for 2 h at 4°C. The membrane was blocked in 5% dried milk in Tris-buffered saline (TBS) plus 0.1% Tween 20 (TBST) for 1 h at room temperature and then probed with polyclonal IRF-3 antibody (Santa Cruz Biotechnology sc-425), VSV whole virus (a gift from John Bell, Ottawa Cancer Centre), Flag M2 (Sigma F3168), Myc (Sigma 9E10), IRF-1 (Santa Cruz Biotechnology sc-9082), IRF-7 (Santa Cruz Biotechnology sc-9083), and actin (Chemicon MAB1501) immunoblotted under the same conditions with concentrations of 1 μg/ml. Incubations were done overnight at 4°C, and incubation mixtures were washed in TBST five times for a total of 25 min. Following washes, the membrane was incubated with peroxidase-conjugated goat anti-rabbit antibody (Amersham) at a dilution of 1:5,000 for 1 h at room temperature. Following the incubation with the secondary antibody, the membrane was washed again for 25 min and then visualized with the enhanced chemiluminescence (ECL) detection system as recommended by the manufacturer (Amersham Biosciences).

Electrophoretic mobility shift assay. Briefly, cell pellets were treated with 10 mM HEPES–50 mM NaCl–10 mM EDTA–5 mM $MgCl_2$–0.5 mM spermidine–0.15 mM spermine–0.5 mM phenylmethylsulfonyl fluoride–10 μg of leupeptin/ml–10 μg of pepstatin/ml–10 μg of aprotinin/ml–1 mM Na_3VO_4. The suspension was held on ice for 30 min and brought to 0.1% NP-40 and 10% glycerol concentrations. Samples were spun for 5 min at 5,000 rpm at 4°C. The supernatant was removed, and the pellet was washed in 50 mM NaCl. Nuclear extracts were obtained in a 10 mM HEPES–400 mM NaCl–0.1 mM EDTA–0.5 mM dithiothreitol (DTT)–0.5 mM phenylmethylsulfonyl fluoride–10 μg of leupeptin/ml–10 μg of pepstatin/ml–10 μg of aprotinin/ml–1 mM Na_3VO_4 solution. Samples were left to rotate at 4°C for 30 min and spun at 15,000 rpm for 10 min at

4°C. WCE were assayed for IRF-3 binding in gel shift analysis with a ^{32}P-labeled double-stranded oligonucleotide corresponding to the ISRE of the IFN-α/β-inducible ISG15 gene (5′-GATCGGAAAGGGAAACCGAAACTGAAGCC-3′). Complexes were formed by incubating the probe with 10 μg of nuclear extract for 20 min at room temperature in 10 mM Tris-Cl (pH 7.5)–1 mM EDTA–50 mM NaCl–2 mM DTT–5% glycerol–0.5% Nonidet P-40–1 μg of bovine serum albumin per μl–1.0 μg of poly(dI-dC)/μl. Extracts were run on a 5% polyacrylamide gel (60:1 cross-link) prepared in 0.25× Tris-borate-EDTA. After being run at 160 V for 3 h, the gel was dried and exposed to a Kodak film at −70°C overnight. To demonstrate the specificity of the detected signal, 1 μg of anti-IRF-3 (Santa Cruz Biotechnology FL-425) or anti-CBP (Santa Cruz Biotechnology sc-369X) antibody was incubated for 30 min on ice prior to the addition of the probe to observe a supershift in the complex formation.

VSV RNP complex isolation. Viral RNP complexes were isolated as previously described (33). Briefly, 5×10^{10} PFU was centrifuged at 30,000 × *g* for 30 min at 4°C. The supernatant was removed, and the viral pellet was resuspended in a low-salt solubilizer solution of 10 mM HEPES (pH 7.5)–5% glycerol–1.85% Triton X-100–0.6 mM DTT–10 U of RNase A–0.3 M NH_4Cl. Following rotation for 2 h at 4°C, the lysed virion mixture was placed on a 30% glycerol cushion and spun at 50,000 × *g* for 90 min in an SW50.1 rotor at 4°C. The bottom pellet was resuspended in 100 μl of water, analyzed by silver staining and spectrophotometry, and tested for remaining infectious particles by standard plaque assay.

RT-PCR. Whole RNA from treated cells was extracted using Trizol (Invitrogen) according to the manufacturer's instructions. RNA purity was analyzed using an Agilent 2000 Bioanalyzer. RT-PCR was performed using 1 μg of RNA resuspended in RNase-free ddH_2O and Oligo dT primer (Clontech) according to the manufacturer's conditions. Reverse transcription was performed using Superscript II (Invitrogen) at 42°C for 1 h. Following the reverse transcription reactions, cDNA samples were brought to 100-μl final volumes of which 5 μl was used as template for each independent PCR with *Taq* polymerase (Amersham). RANTES fragments were amplified with 5′-ATCTCGAACTCCTGACCTCAA GTAATCC-3′ and 5′-TACACCAATGGCAAGTGCTCCAACCCAG-3′, and actin fragments were amplified with 5′-ACAATGAGCTGCTGGTGGCT-3′ and 5′-GATGGGCACAGTGTGGGTGA-3′ primers at an annealing temperature of 60°C. RT-PCR products were run on a 2% agarose gel and revealed through use of a Typhoon 9400 phosphoimager (Amersham).

In vitro kinase assay. Immunoprecipitations for the in vitro kinase assay were performed by incubating WCE (150 μg) for 4 h at 4°C with protein A-Sepharose beads (Amersham Pharmacia, Uppsala, Sweden) precoupled to specific antisera directed against TBK1 (rabbit polyclonal antibody; a kind gift from Tom Maniatis, Harvard University). The precoupling reaction was performed by incubation of 0.5 μg of specific antisera per 30 μl of packed Sepharose beads for 2 h at 4°C in TNET buffer (50 mM Tris [pH 7.4], 100 mM NaCl, 1 mM EDTA [pH 8.0], 0.5% NP-40) containing 1% bovine serum albumin. Immunocomplexes were washed twice in lysis buffer and twice in a standard IKK kinase buffer (20 mM HEPES, 10 mM $MgCl_2$, 0.1 mM sodium orthovanadate, 20 mM β-glycerophosphate, 10 mM *p*-nitrophenylphosphate, 1 mM DTT, and 50 mM NaCl). The kinase reaction was performed by incubation of immunocomplexes with 1× kinase buffer–10 μCi of [γ-^{32}P]ATP–1 mM ATP–0.5 to 1.0 μg of GST substrate at 30°C for 30 min in a 40-μl volume. Following fractionation of samples by SDS–10% PAGE, the upper half of the gel was transferred to a nitrocellulose membrane and blotted for immunoprecipitated kinase; the lower half of the gel was stained with Coomassie blue for 15 min, destained in 10% methanol–10% acetic acid for 1 h, soaked in 2% glycerol for 30 min, dried, and exposed to Biomax XR film (Kodak).

Preparation of baculovirus-expressed IKKε and TBK1. Vectors for production of recombinant baculoviruses were generated by subcloning IKKε and TBK1 cDNAs into the pAcH6N1 vector. For preparation of purified recombinant IKKε and TBK1, 15-cm-diameter tissue culture plates were seeded with 2×10^7 Sf9 insect cells (BD Biosciences) per plate. Fresh TMN-FH medium (BD Biosciences) containing 10% heat-inactivated FBS was added to make up a final volume of 30 ml per plate. Sf9 cells were infected (multiplicity of infection [MOI] of >1.0) with a high-titer stock solution of recombinant baculoviruses integrated with human TBK1 and IKKi cDNA (minimum titer, 10^8 virus particles/ml). Following incubation at 27°C for 3 days, the cells were harvested by centrifugation at 2,500 rpm for 10 min. Following resuspension of the cell pellet with 1 ml of cold lysis buffer (50 mM Tris [pH 7.5], 650 mM NaCl, 5% Triton X-100, 50 mM NaF, 50 mM NaP_i [pH 7.5], 50 mM $NaPP_i$ [pH 7.5]), the lysate was incubated on ice for 1 h and centrifuged at 13,000 rpm for 30 min. The supernatant was incubated with His-binding beads (Novagene; 0.5 ml of supernatant per 50 μl of beads) preequilibrated with His binding buffer for 1 h at 4C. Beads were washed with His washing buffer three times, and recombinant proteins were eluted in His eluting buffer for 30 min at 4°C. Control and purified kinase extract (500 ng) was used in a standard IKK in vitro kinase assay as described above.

Luciferase assay. Subconfluent cells in 35-mm-diameter tissue culture dishes were transfected with 20 ng of pRLTK reporter (*Renilla* luciferase for internal control) and 100 ng of pGL3 reporter (firefly luciferase, experimental reporter) with use of Lipofectamine 2000 (Invitrogen) as detailed by the manufacturer. Cells were harvested 24 h posttransfection, lysed in passive lysis buffer (Promega), and assayed for dual-luciferase activity with use of 5 μl of lysate according to the manufacturer's instructions. All firefly luciferase values were normalized to *Renilla* luciferase to control for transfection efficiency, and results shown represent the averages of at least three independent experiments.

RESULTS

VSV-induced activation of the antiviral state. Initially, a time course analysis of VSV infection was performed in the human epithelial A549 cell model to determine the kinetics of the IFN response to virus infection. A549 cells, infected with VSV at an MOI of 10.0, were harvested at various times from 0 to 48 h postinfection (hpi); WCE (50 μg) were submitted to one-dimensional gel electrophoresis and immunoblotted with antisera to IRF-3, IRF-3 S396P, IRF-7, IRF-1, ISG56, actin, and VSV (Fig. 1A). C-terminal phosphorylation of IRF-3 following VSV infection was observed between 8 and 24 h, as detected by the appearance of the phosphoforms III and IV (Fig. 1A, lanes 3 to 7). In addition to the slower-migrating forms, IRF-3 phosphorylation was also confirmed using the Ser396 phosphospecific antibody (Fig. 1A, lanes 3 to 7) (47). At 24 hpi IRF-3 phosphorylation was decreased, based on the phosphospecific S396 IRF-3 antibody and the disappearance of forms III and IV (Fig. 1A, lanes 8 and 9). Throughout the course of VSV infection, the induction of the IRF-3-responsive gene ISG56 and IFN-responsive genes such as those for IRF-1 and IRF-7 was also observed (Fig. 1A, lanes 4 to 9). RT-PCR demonstrated that induction of IRF-3-dependent RANTES mRNA (11, 23) was observed as early as 8 hpi and was sustained for the duration of the infection kinetics (Fig. 1A, bottom panel, lanes 3 to 9); similar results were obtained for IFN-β mRNA expression (data not shown).

To demonstrate nuclear translocation and DNA binding, nuclear extracts were analyzed for IRF-3 binding to the ISRE of the ISG15 gene. Phosphorylation of the IRF-3 C terminus, as observed by induction of forms III and IV and S396 phosphorylation, correlated with the ability of IRF-3 to bind DNA (Fig. 1A and B, lanes 3 to 8). Infection by VSV induced two specific complexes on the ISG15 ISRE (54), which represent IRF-3 and IRF-3 bound to CBP (Fig. 1B, lanes 3 to 7). Binding was detected at 8 hpi and increased until 24 hpi (Fig. 1B, lanes 3 to 7). At 36 and 48 hpi, binding of IRF-3 to the ISRE was no longer detected, which correlated with decreased IRF-3 phosphorylation (Fig. 1B, lanes 8 and 9). These data demonstrate that VSV infection induces the phosphorylation and activation of IRF-3 and the transcriptional upregulation of immunomodulatory genes such as IRF-1, ISG56, IRF-7, and RANTES during the course of VSV infection of A549 cells.

VSV-induced IRF-3 activation is MOI dependent and requires virus replication. Next, VSV infection at different MOIs was performed and analyzed by SDS-PAGE and immunoblotting. VSV infection at MOIs of 0.1, 1.0, 10, and 100 was performed in A549 cells, and cells were harvested at 0, 2, 4, and 6 hpi (Fig. 2A). At an MOI of 0.1 or 1.0, no IRF-3 phosphorylation was observed within the first 6 h of infection (Fig. 2,

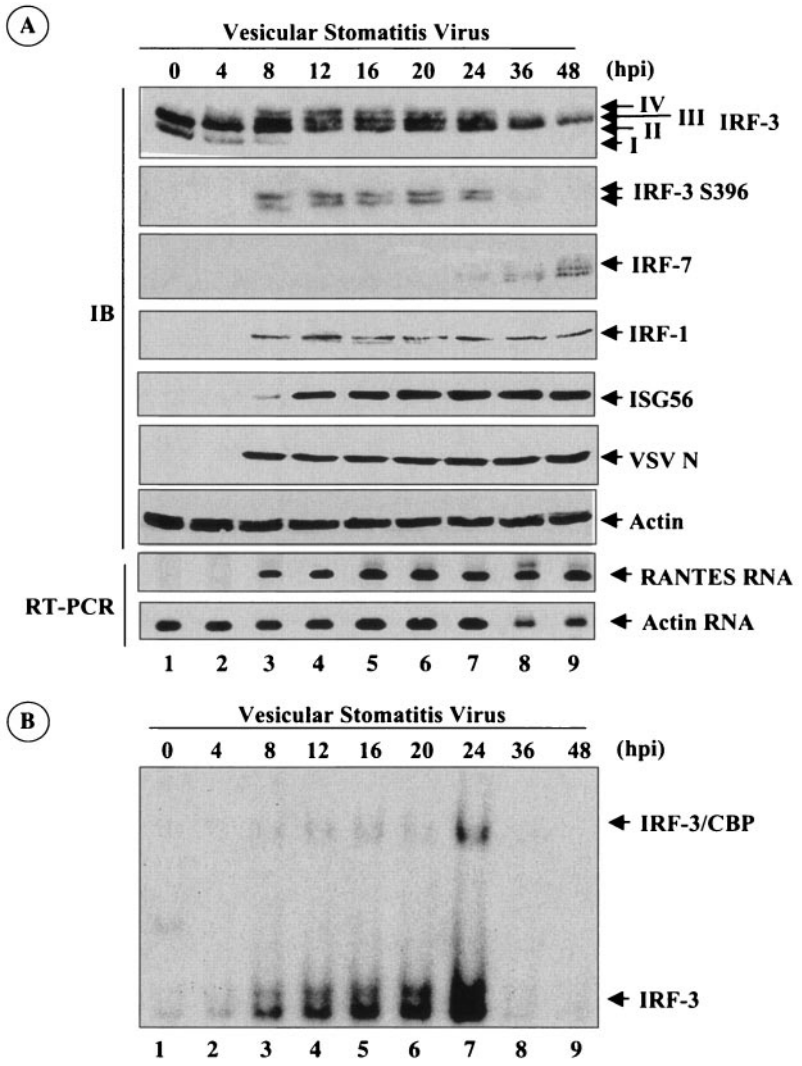

FIG. 1. VSV-induced activation of the antiviral state. (A) WCE (50 μg) prepared from A549 cells infected with VSV (MOI of 10.0) from 0 to 48 hpi was resolved by SDS–7.5% PAGE and transferred to nitrocellulose. IRF-3, IRF-3 S396, IRF-7, IRF-1, ISG56, VSV proteins, and actin were detected by immunoblotting with specific antisera. VSV nucleocapsid protein is denoted by N. Additionally, A549 whole-cell RNA extract was obtained from a duplicate experiment for RT-PCR analysis of RANTES and actin as indicated. (B) WCE as outlined above was used to analyze IRF-3 binding activity by electrophoretic mobility shift assay with the ISRE of the ISG15 probe. Arrows indicate complexes of IRF-3 and IRF-3/CBP.

lanes 1 to 8). At an MOI of 10, IRF-3 activation was detectable at 4 to 6 hpi, which correlated with the appearance of the VSV nucleocapsid (N) protein (Fig. 2, lanes 11 and 12); at an MOI of 100, VSV induced IRF-3 phosphorylation by 4 hpi (Fig. 2, lanes 15 and 16). To evaluate whether virus transcription and/or translation was required for IRF-3 phosphorylation, VSV infection (MOI of 10) was performed in the presence or absence of either ribavirin, an inhibitor of RNA-dependent RNA polymerase (RdRp) transcription (35), or cycloheximide, an inhibitor of translation (10), for 0 to 6 hpi (Fig. 2B). Ribavirin treatment blocked IRF-3 phosphorylation (Fig. 2B, lanes 6 to 8), demonstrating the requirement for VSV transcription, as previously established with other single-stranded RNA viruses (48, 51, 54), To ensure that ribavirin treatment inhibited the primary transcription of VSV, the expression of VSV N protein and VSV N mRNA was evaluated through immunoblotting and RT-PCR analysis, respectively. Neither VSV N protein nor mRNA was detected in the presence of ribavirin, indicating a complete block in RdRp activity (Fig. 2B, two middle panels, lanes 6 to 8). Similarly, treatment with cycloheximide induced an IRF-3 shift from form I to form II in the absence of virus infection (Fig. 2B, lane 13) (48), but VSV infection in the presence of cycloheximide failed to induce IRF-3 form III or IV (Fig. 2B, lanes 6 to 8). This experiment suggested that VSV primary transcription and de novo translation of VSV are required for the induction of C-terminal IRF-3 phosphorylation.

Differential induction of IRF-3 phosphorylation by VSV infection, dsRNA, and RNP. Based on the above results and previous observations with Sendai and measles virus models (48, 54), we hypothesized that intracellular accumulation of VSV RNP complex may be recognized by a pathway leading to

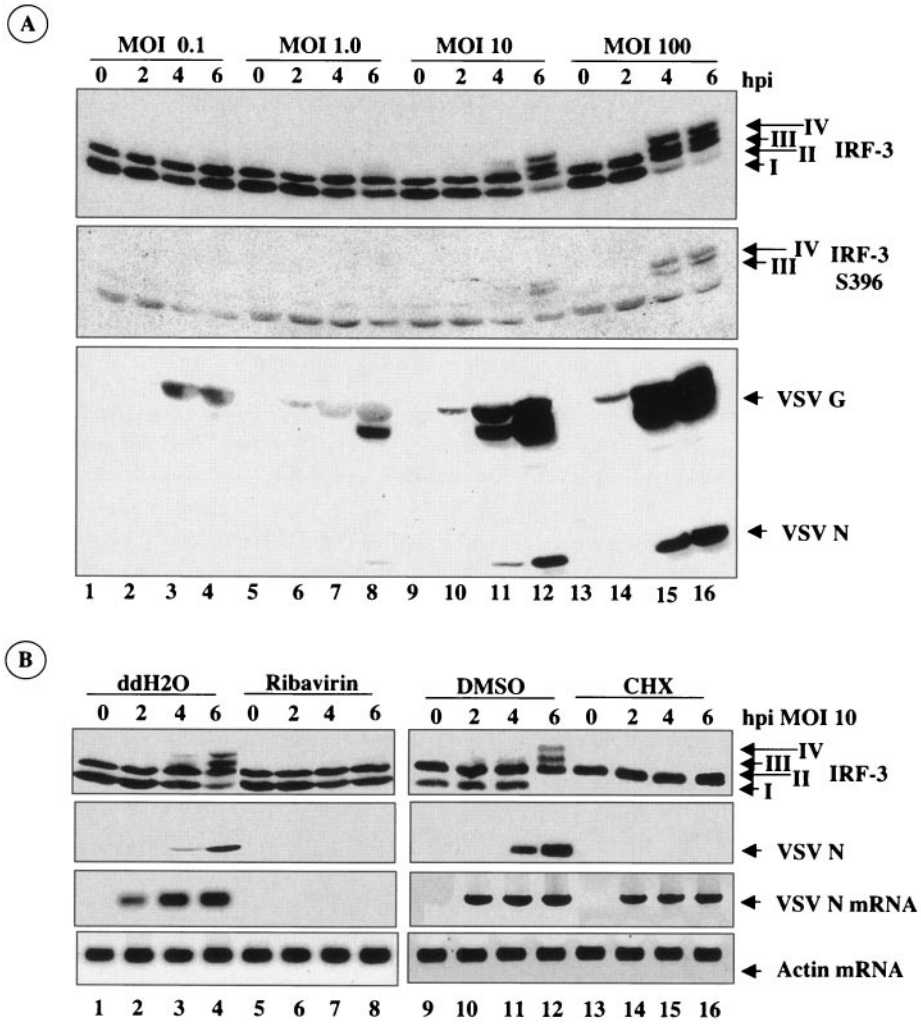

FIG. 2. VSV-induced IRF-3 phosphorylation is MOI dependent and requires virus replication. (A) A549 cells were treated with VSV at MOIs of 0.1, 1.0, 10, and 100 for 0, 2, 4, and 6 hpi as indicated. WCE (50 μg) was analyzed by SDS–7.5% PAGE, transferred to nitrocellulose, and immunoblotted for IRF-3, IRF-3 S396, and antisera to VSV. (B) A549 cells were pretreated with ddH_2O, DMSO, cycloheximide (CHX; 100 μg/ml), or ribavirin (500 μg/ml) 30 min prior to VSV infection (MOI of 10). WCE was analyzed by SDS–7.5% PAGE, transferred to nitrocellulose, and immunoblotted for IRF-3 and VSV antisera (N denotes nucleocapsid protein). RNA isolated from duplicate samples was subjected to RT-PCR and analyzed using specific primers for VSV N and actin.

IRF-3 activation. To test this idea, the VSV RNP complex was purified from VSV virions (33), transfected into A549 cells, and compared to de novo VSV infection and dsRNA [poly(I) · poly(C)] transfection with respect to IRF-3 activation (Fig. 3). VSV RNP induced IRF-3 phosphorylation as effectively as did either VSV infection (MOI of 100, 6 hpi) or dsRNA; the S396 phosphospecific antibody confirmed the C-terminal phosphorylation of IRF-3 (Fig. 3A, top two panels, lanes 2 to 4). Furthermore, both IRF-1 and ISG56 expression were induced in response to VSV or RNP but were only weakly induced by dsRNA; with dsRNA as inducer, a weaker phosphorylation of Ser396 than that with VSV or RNP was also observed (Fig. 3A, middle panels, lanes 2 to 4). To ensure that VSV RNP transfection did not induce viral infection, immunoblotting against VSV proteins demonstrated that only VSV infection produced VSV G and N proteins (Fig. 3A, lane 2); thus, purified RNP was transcriptionally inert. Additionally, VSV RNP preparations were evaluated for infectivity by a standard plaque assay and demonstrated that VSV RNP did not induce plaque formation (data not shown). The DNA binding capacity of IRF-3 in response to VSV, dsRNA, or RNP was also tested (Fig. 3B). As expected, IRF-3 and IRF-3/CBP complexes were induced following VSV infection or transfection of dsRNA or RNP (Fig. 3B, lanes 2 to 4).

Since minute levels of the L and P subunits of the VSV RdRp have been reported to fractionate during RNP isolation (33), an experiment was performed to ensure that RNP-dependent IRF-3 activation was not dependent on VSV polymerase activity. A549 cells were treated with ribavirin or cycloheximide prior to RNP transfection to evaluate whether blocking RdRp transcription or translation could inhibit RNP-induced IRF-3 activation. Regardless of treatment, IRF-3 phosphorylation was detected at 6 h post-RNP transfection (Fig. 3C, lanes 2 to 4). Furthermore, the IRF-3-responsive ISG56 pro-

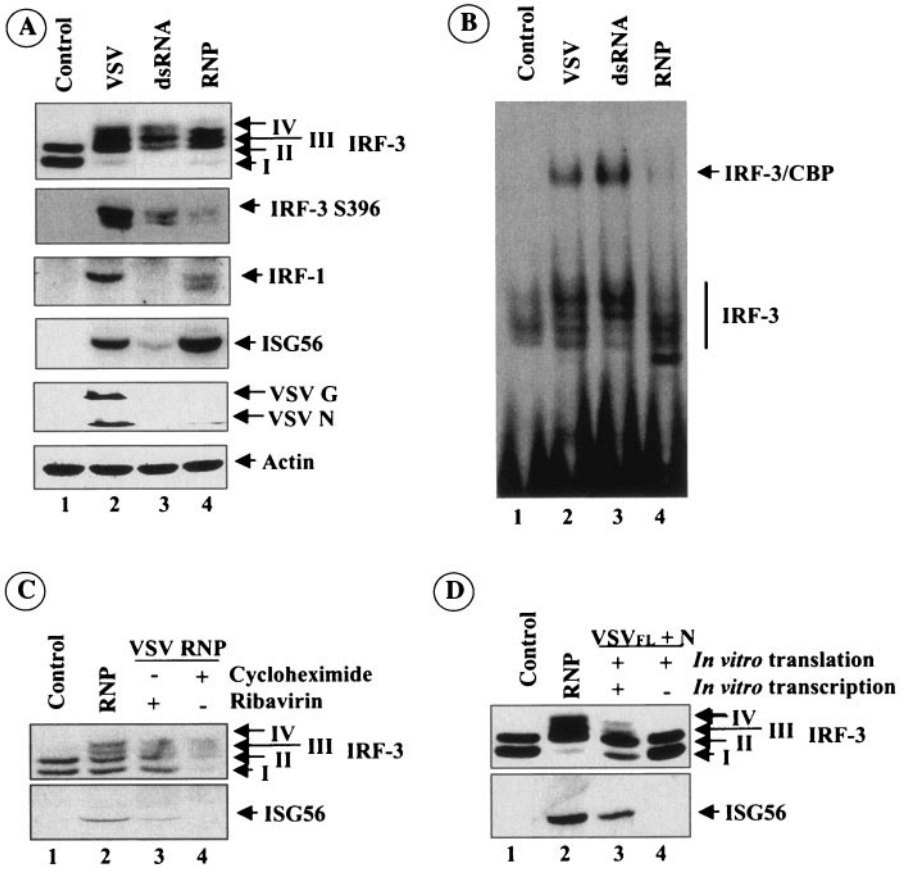

FIG. 3. VSV infection, dsRNA, or RNP induces an antiviral response. (A) A549 cells were treated with either vector alone, vector and VSV (MOI of 10), dsRNA, or RNP for 6 h. WCE (50 μg) was analyzed by SDS–7.5% PAGE, transferred to nitrocellulose, and immunoblotted for IRF-3, IRF-3 S396, IRF-1, ISG56, VSV antisera, or actin as indicated. (B) WCE (5 μg) as outlined was used to analyze IRF-3 binding activity by electrophoretic mobility shift assay with the ISRE of the ISG15 probe. Arrows indicate the protein-DNA complexes of IRF-3 and IRF-3/CBP. (C) A549 cells were pretreated with vehicle (ddH_2O or DMSO), ribavirin (500 μg/ml), or cycloheximide (100 μg/ml) 30 min prior to RNP treatment as indicated. WCE (30 μg) was analyzed by SDS–7.5% PAGE, transferred to nitrocellulose, and immunoblotted for IRF-3 and ISG56. (D) In vitro transcriptions either alone or coupled to in vitro translation of VSV N cDNA and VSV genome cDNA were transfected into A549 cells and compared to de novo isolated RNP transfection for 6 h. WCE (60 μg) was analyzed by SDS–7.5% PAGE, transferred to nitrocellulose, and immunoblotted for IRF-3 and ISG56 as indicated.

tein was induced in the presence of ribavirin (Fig. 3C, lane 3), but synthesis was blocked by the protein synthesis inhibitor cycloheximide (Fig. 3C, lane 4).

As an additional control to demonstrate that VSV RNP could induce IRF-3 activation independently of RdRp activity, synthetic RNP was generated by de novo transcription and translation of VSV N cDNA (pBS-VSV N) and the cDNA of the VSV genome (pBS VSV FL) as previously described (33). Two independent reactions were performed; one reaction mixture was subjected to T7 polymerase transcription, and the other reaction mixture was transcribed and translated using a rabbit reticulocyte lysate. A cycloheximide-treated rabbit reticulocyte lysate was also added to the in vitro transcription reaction mixture as an additional control. The transcribed and translated products were transfected into A549 cells and analyzed for IRF-3 and ISG56 at 6 h (Fig. 3D). Although de novo purified VSV RNP was the strongest inducer of IRF-3 phosphorylation and ISG56 induction (Fig. 3D, lane 2), in vitro-transcribed and -translated RNP was also able to induce IRF-3 phosphorylation and ISG56 expression (Fig. 3D, lane 3). However, in vitro transcription of the VSV genome and N mRNA in the absence of VSV N translation failed to induce IRF-3 phosphorylation (Fig. 3D, lane 4), thus reflecting the requirement for intact RNP complexes.

Activation of TBK1 in response to VSV infection, dsRNA, and RNP. Since TBK1 is the critical kinase upstream of IRF-3 phosphorylation, we investigated whether RNP and dsRNA induced the catalytic activity of TBK1 in a manner similar to that of virus infection (Fig. 4). All three stimuli induced TBK1 kinase activity in A549 cells, as demonstrated by specific phosphorylation of a GST-IRF-3(aa380-427) peptide substrate (compare Fig. 4, control lanes 1 to 6, with lanes 10 to 12, 13 to 18, and 22 to 24, upper panel). Comparable levels of TBK1 were immunoprecipitated in each reaction (Fig. 4, middle panels), and for all three stimuli, induction of TBK1 kinase activity in vitro correlated with the appearance of phosphorylated forms III and IV of IRF-3 in vivo (Fig. 4, bottom panels). Significant differences with respect to the kinetics of TBK1 activation were observed; dsRNA treatment resulted in rapid induction of TBK1 kinase activity, as early as 1 h posttransfec-

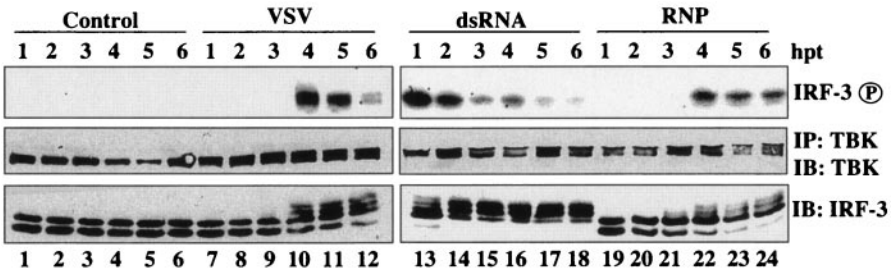

FIG. 4. Activation of TBK1 kinase activity by VSV infection, dsRNA, or RNP complex. A549 cells were treated with vehicle (Control), VSV (MOI of 100), dsRNA, or VSV RNP for the time points indicated. WCE (1 mg) was immunoprecipitated with anti-TBK1 antisera, and following washing, the immunoprecipitate was assayed for IRF-3 kinase activity (top panels) or transferred to nitrocellulose and immunoblotted for TBK1 expression to ensure equal binding (middle panels). Additionally, duplicate WCE (50 μg) were analyzed by Western blotting to detect IRF-3 phosphorylation (bottom panel). hpt, hours posttreatment.

tion (Fig. 4, lane 13, upper panel). Importantly, both VSV infection and RNP treatment activated TBK1 with identical kinetics, detectable in the kinase assay at 4 h poststimulation (Fig. 4, lanes 10 and 22, upper panel, respectively). Together, these data demonstrate that VSV infection, ribonucleoprotein complexes, and dsRNA can activate TBK1 activity, IRF-3 phosphorylation, and induction of the IFN antiviral response, although, based on the kinetics of kinase activation, dsRNA potentially uses a pathway that is distinct from that used by VSV or RNP.

VSV infection induces IRF-3 phosphorylation independently of TLR3 and TRIF. Since TBK1 and IKKε are downstream of dsRNA-TLR3 signaling (8, 30), we sought to determine whether TLR3 or TRIF was required for VSV- and/or dsRNA-induced IRF-3 phosphorylation. Control MEFs or MEFs derived from targeted gene disruption of TLR3 were infected with VSV or transfected with poly(I) · poly(C) and harvested 0 to 6 h posttreatment (Fig. 5A and B). VSV infection induced IRF-3 phosphorylation at 4 h after infection in both wt MEFs and TLR3$^{-/-}$ MEFs (Fig. 5A, lanes 2 to 4 and 6 to 8). Surprisingly, poly(I) · poly(C) transfection induced IRF-3 phosphorylation, regardless of the presence or absence of TLR3 (Fig. 5B, lanes 2 and 6). However, unlike IRF-3 phosphorylation in response to VSV, dsRNA induced rapid IRF-3 phosphorylation at 2 h, a response that was followed by IRF-3 degradation (Fig. 5B, lanes 3 and 4 and lanes 7 and 8). In other preliminary studies, virus infection led to the activation of the IFN-β promoter in TRIF$^{-/-}$ fibroblasts, indicating that activation by virus was independent of TRIF (data not shown). Taken together, these results demonstrate that VSV and transfected dsRNA, unlike simple overlay of dsRNA, induce IRF-3 C-terminal phosphorylation independently of TLR3 expression. Furthermore, IRF-3 phosphorylation was also detected in VSV-infected MEFs derived from TRIF-deficient mice and compared to the TLR3$^{-/-}$ MEFs (Fig. 5C, lanes 2 and 4, respectively). This observation demonstrates that, in the absence of TLR3 and TRIF signaling components, VSV was able to induce IRF-3 phosphorylation in a TLR3- and TRIF-independent manner.

IKKε expression partially compensates for TBK1 deficiency. Next TBK1$^{+/+}$ or TBK1$^{-/-}$ MEFs (3) were infected with VSV (MOI of 10) or transfected with either dsRNA or purified RNP for 0 to 9 h, to determine whether IRF-3 activation was impaired in the absence of TBK1. WCE from TBK1$^{+/+}$ cells showed IRF-3 phosphorylation within 6 h of VSV infection, 3 h following dsRNA transfection, or 6 h post-RNP transfection (Fig. 6A, lanes 3, 6, and 11, respectively). Interestingly, expression of the closely related IKKε was induced by VSV, dsRNA, or RNP treatment within 3 h poststimulation (Fig. 6A, lanes 2, 6, and 10). In contrast, IRF-3 phosphorylation in TBK1$^{-/-}$ MEFs infected with VSV or treated with dsRNA or RNP was dramatically reduced compared to that in TBK1$^{+/+}$ cells (Fig. 6B). In both TBK1$^{+/+}$ and TBK1$^{-/-}$ MEFs, induction of IKKε expression was intact and was stimulated at 3 h after VSV, dsRNA, or RNP treatment, essentially as observed in TBK1$^{+/+}$ cells (Fig. 6B, lanes 2, 6, and 10).

To determine whether the reduction in IRF-3 phosphorylation in TBK1$^{-/-}$ MEFs was also reflected in a decrease in IRF-dependent transcription, reporter gene assays with the ISRE-driven RANTES promoter lacking NF-κB responsiveness (κBm RANTES) were evaluated (23) (Fig. 7). VSV infection (MOI of 0.1) induced >9-fold induction of the κBm RANTES promoter in TBK1$^{+/+}$ MEFs, whereas in TBK1$^{-/-}$ MEFs, induction was decreased to <3-fold. This result suggests that activation of TBK1 is required to achieve robust activation of IRF-3 following virus infection (Fig. 7). κBm RANTES-driven luciferase levels were low in both TBK1$^{+/+}$ and TBK1$^{-/-}$ MEFs, and stimulation with dsRNA or RNP yielded values too low to be statistically analyzed following standardization (data not shown). Also, the IRF-7 expression construct and the IFNA4 promoter construct were transfected into TBK1$^{+/+}$ and TBK1$^{-/-}$ MEFs and infected with VSV (MOI of 0.1) or treated with dsRNA or RNP for 16 h. In TBK1$^{+/+}$ MEFs, VSV, dsRNA, and RNP stimulated 18-, 24-, and 6-fold induction of the IRF-7-dependent IFNA4 promoter, respectively (Fig. 7), whereas in TBK1$^{-/-}$ MEFs, IFNA4 activity was diminished 11-, 13-, and 1.4-fold, respectively, suggesting that TBK1 was also required for full IRF-7 activation (Fig. 7). Thus, TBK1 expression is required for full induction of IRF-3 and IRF-7 as previously demonstrated. However, induction of IKKε expression in response to VSV, dsRNA, and RNP may contribute to kinase activity that in part compensates for the absence of TBK1 and induces IRF-3 and IRF-7 activity.

TBK1 and IKKε demonstrate redundancy with respect to IRF-3 and IRF-7 C-terminal phosphorylation. The IRF-3 carboxyl terminus (aa 380 to 427 region) (Fig. 8A) contains sev-

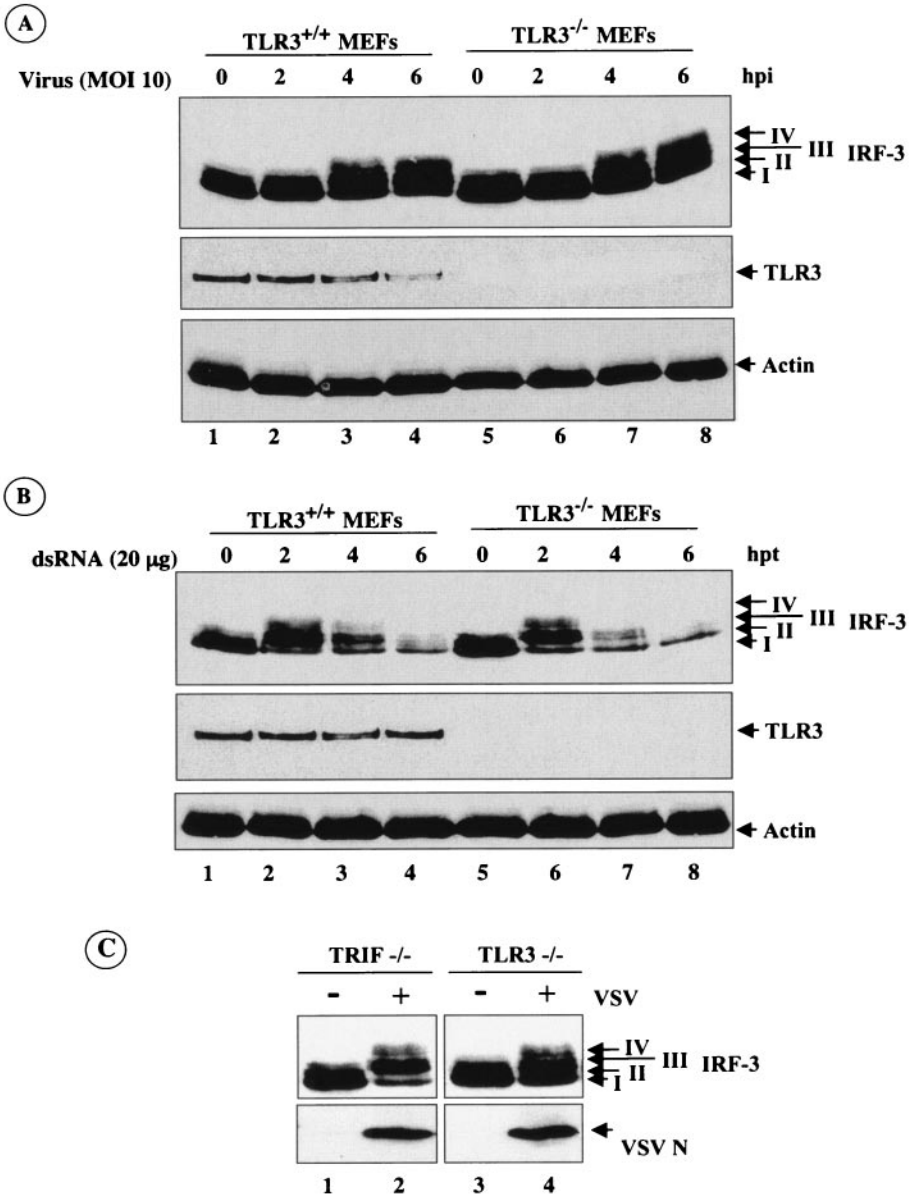

FIG. 5. VSV infection induces IRF-3 phosphorylation in the absence of TLR3 or TRIF. (A) C57/BL TLR3$^{-/-}$ MEFs and wt control MEFs were infected with VSV (MOI of 10) or treated with poly(I) · poly(C) dsRNA for 0 to 6 h. WCE (50 μg) derived from VSV-infected cells were analyzed by SDS–7.5% PAGE; transferred to nitrocellulose; and blotted for IRF-3, TLR3, and actin as indicated. (B) WCE (50 μg) derived from dsRNA-treated TLR3$^{-/-}$ MEFs and wt control MEFs were analyzed as described for panel A. (C) WCE (40 μg) prepared from TRIF$^{-/-}$ or TLR3$^{-/-}$ MEFs were infected with VSV (MOI of 10) for 9 h and immunoblotted for IRF-3 and VSV N as indicated. hpt, hours posttreatment.

eral serine and threonine residues that are important for full activation of IRF-3 in response to virus infection (24, 26, 47, 58). The seven residues are grouped into two distinct clusters, a two-residue 385-386 cluster at the amino terminus of the IRF-3 transactivation domain (cluster I) and a five-residue 396 to 405 cluster at the carboxy terminus of the transactivation domain (termed the 5S/T cluster II). Six GST-IRF-3(aa380-427) peptide mutants were constructed to introduce specific Ser- or Thr-to-Ala mutations. Equal amounts of recombinant IKKε and TBK1 purified from baculovirus-infected Sf9 cells were used in a standard in vitro kinase assay with the wt and the GST-IRF-3(aa380-427) peptides as substrates (Fig. 8A). Both TBK1 and IKKε directly phosphorylate IRF-3 within the carboxyl terminus (Fig. 8A, lanes 1 and 8), although TBK1 activity was consistently higher. The two kinases exhibited an identical pattern of direct IRF-3 carboxy-terminal phosphorylation (Fig. 8A, compare lanes 1 to 7 with lanes 8 to 14). Mutation of the seven critical C-terminal residues abolished IRF-3 phosphorylation by IKKε or TBK1 (Fig. 8A, lanes 2 and 9). Mutation of the cluster II serine/threonine residues to alanine diminished >90% of the IKKε- or TBK1-mediated IRF-3 phosphorylation (Fig. 8A, lanes 3 and 10), clearly demonstrat-

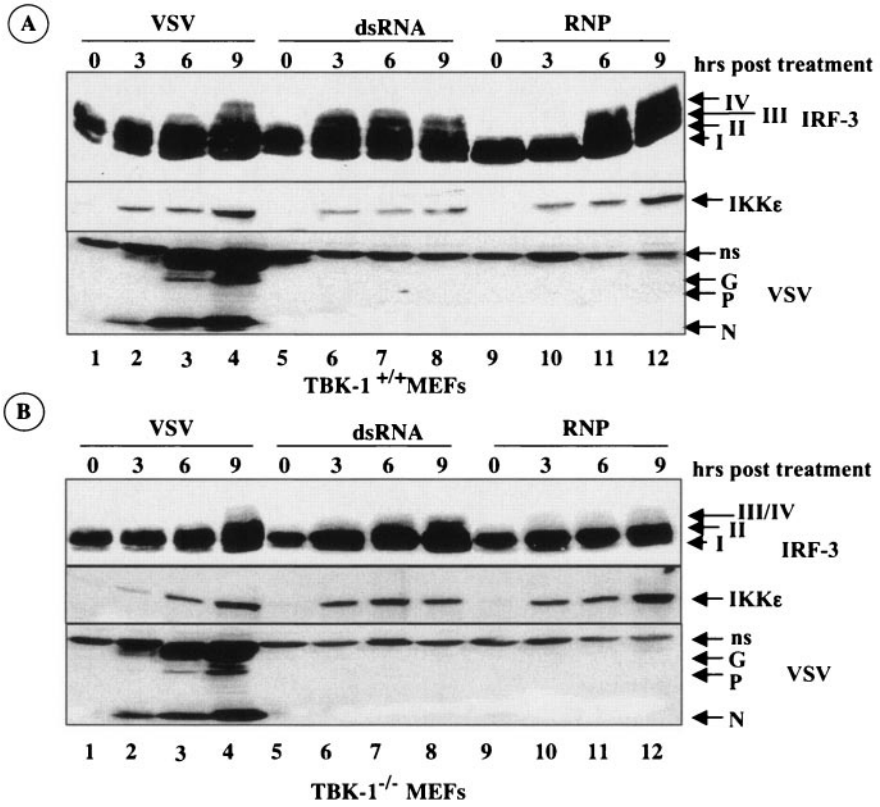

FIG. 6. Defective IRF-3 activation in TBK1$^{-/-}$ MEFs. (A) C57/BL wt MEFs were treated with VSV (MOI of 10), dsRNA, or RNP for 0, 3, 6, and 9 h. WCE (55 μg) were analyzed by SDS–7.5% PAGE, transferred to nitrocellulose, and immunoblotted for murine IRF-3, IKKε, and VSV (ns, G, P, and N denote nonspecific, VSV glycoprotein, VSV phosphoprotein, and VSV nucleocapsid protein, respectively). (B) C57/BL MEFs disrupted in TBK1 gene expression were treated and analyzed as described for panel A.

ing that the cluster II residues within the IRF-3 C terminus are the primary targets for phosphorylation by IKKε and TBK1.

The specific S402A mutation within the 5S/T cluster was associated with the loss of a majority of IRF-3 phosphorylation by TBK1 and IKKε (Fig. 8A, lanes 4, 6, 10, and 12). The position of S402 as the second residue within a mitogen-activated protein kinase–IKK SerXXXSer recognition motif (Fig. 8A) is consistent with the target motif previously documented

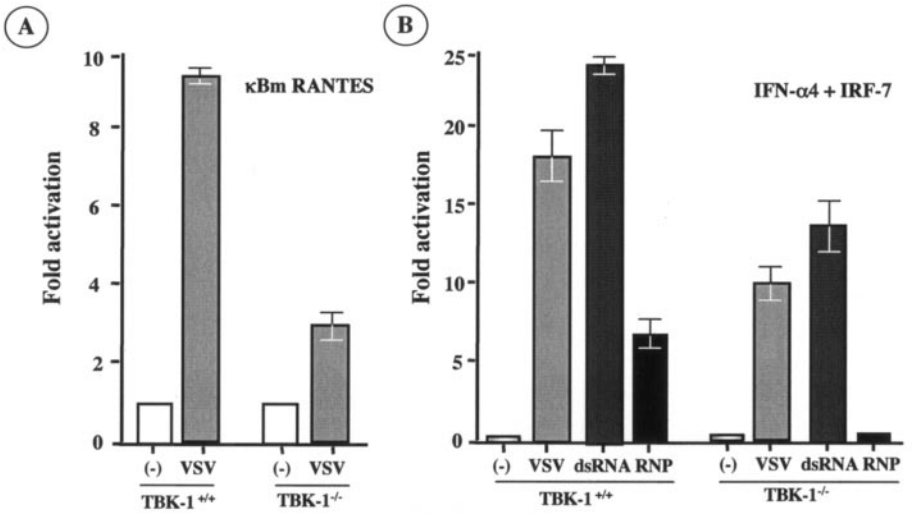

FIG. 7. Reduced RANTES and IFNA4 expression in TBK1$^{-/-}$ MEFs. (A) C57/BL TBK1$^{+/+}$ and TBK1$^{-/-}$ cells were transfected with a luciferase reporter plasmid encoding the κBm RANTES promoter and treated with VSV for 16 h (MOI of 0.1). (B) C57/BL TBK1$^{+/+}$ and TBK1$^{-/-}$ cells were transfected with an IFNA4 promoter luciferase plasmid and an IRF-7 expression plasmid. Luciferase activities were expressed as fold activation relative to the basal level; values represent the averages of two experiments, performed in duplicate.

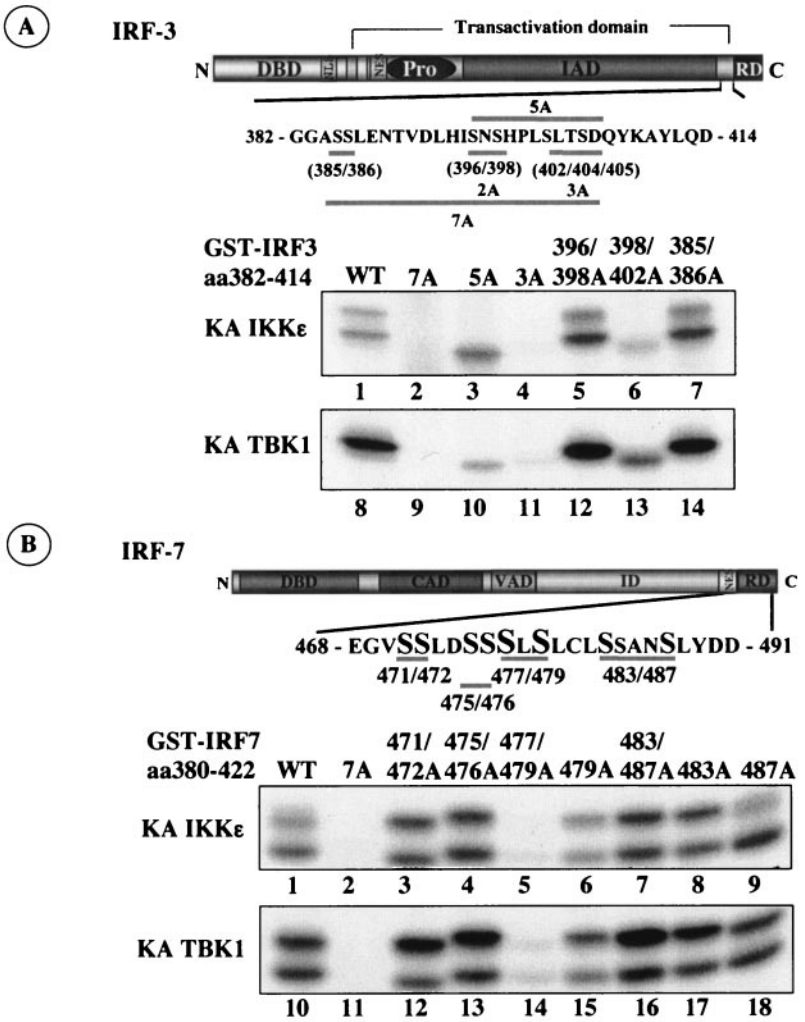

FIG. 8. Purified TBK1 and IKKε kinases share identical IRF-3 and IRF-7 substrate specificities. (A) Schematic representation of IRF-3. Positions of the DNA binding domain (DBD), nuclear localization sequence (NLS), nuclear export sequence (NES), proline-rich domain (Pro), IRF interaction domain (IAD), and regulatory domain (RD) are indicated. Recombinant TBK1 (0.5 μg, lanes 8 to 14) and IKKε (0.5 μg, lanes 1 to 7) purified from baculovirus-infected Sf9 insect cells were used for in vitro kinase analysis of wt and S/T-to-A mutants of GST-IRF-3(aa380-427). Kinase reactions were resolved by SDS–10% PAGE and analyzed by autoradiography; positions of phosphorylated GST-IRF-3 are indicated. (B) Schematic representation of IRF-7. Positions of the DNA binding domain (DBD), constitutive activation domain (CAD), virus activation domain (VAD), regulatory domain (RD), and nuclear export signal (NES) are indicated. GST-IRF-7(aa468-503) peptide substrates are detailed. Recombinant TBK1 (0.5 μg, lanes 10 to 18) and IKKε (0.5 μg, lanes 1 to 9) purified from baculovirus-infected Sf9 insect cells were used for in vitro kinase analysis of wt and S/T-to-A mutants of GST-IRF-7(aa468-503) peptide substrates. Kinase reactions were resolved by SDS–10% PAGE and analyzed by autoradiography; positions of phosphorylated GST-IRF-7 are indicated.

for TBK1 and IKKε in the amino-terminal domain of IκBα (17, 20, 36, 50).

Next, to determine which of the C-terminal residues within IRF-7(aa468-491) are directly targeted by the IKK-related kinases, peptide substrates corresponding to the wt and eight Ser-to-Ala mutants of GST-IRF-7 were analyzed by in vitro kinase assay with purified IKKε and TBK1 (Fig. 8B). GST-IRF-7(aa468-503) is phosphorylated more efficiently by TBK1 than is IKKε (Fig. 8B, compare lanes 1 and 8); moreover, the two kinases exhibit an identical specificity with respect to direct IRF-7 C-terminal phosphorylation (Fig. 8B, compare lanes 1 to 9 with lanes 10 to 18). Mutation of seven residues within the aa 475 to 487 domain abolished TBK1- and IKKε-mediated phosphorylation of IRF-7 (Fig. 8B, lanes 2 and 11). Similarly, an S477/479A mutation decreased ~80% of direct IRF-7 phosphorylation by IKKε and TBK1 (Fig. 8B, lanes 5 and 10), while a mutation of S479A reduced phosphorylation by approximately 50%. Based on these results, the Ser477 and Ser479 residues appear to be the primary target for phosphorylation by IKKε and TBK1. The position of Ser479 within the IRF-7 carboxyl terminus is consistent with the SXXXS consensus motif; however, the S479A mutation did not completely abolish direct phosphorylation by TBK1 and IKKε, presumably due to phosphorylation at Ser477.

In an effort to correlate the IRF-7 in vitro phosphorylation with transactivation potential, full-length IRF-7 Ala point mutations (Fig. 8B) were generated and cotransfected into 293 HEK cells together with an IFNA4 promoter construct. Coex-

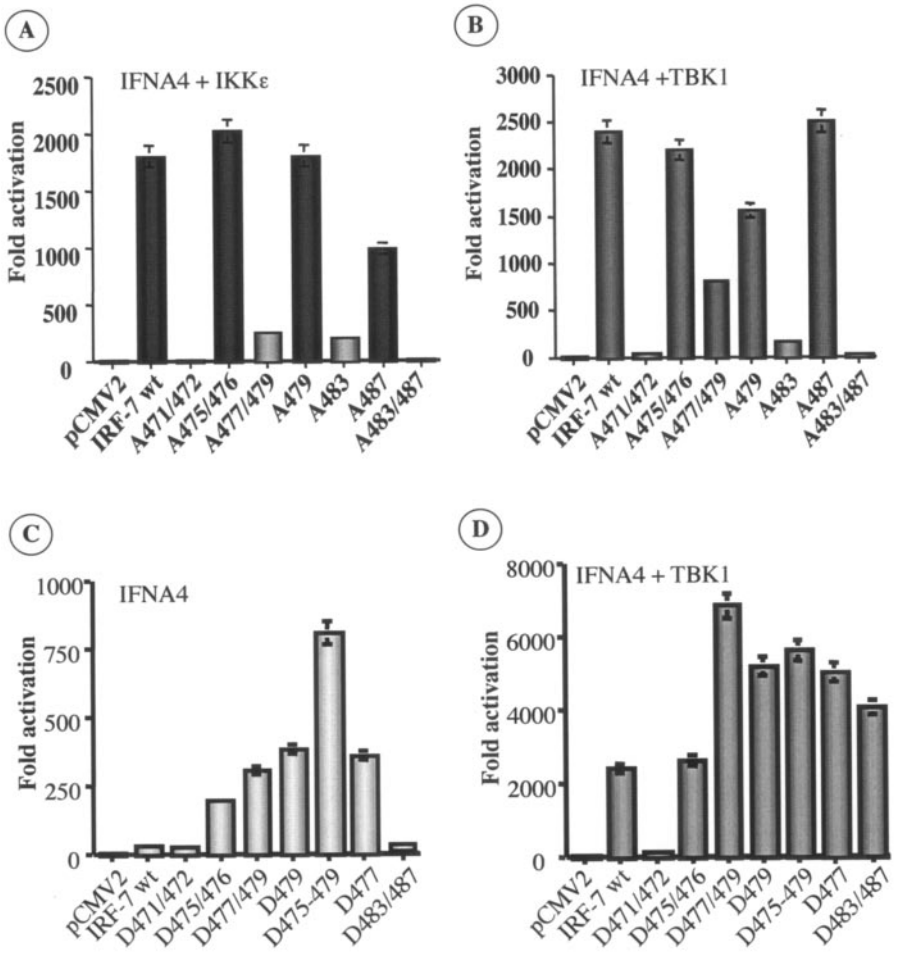

FIG. 9. Activation of the IFNA4 promoter by wt and point mutations of IRF-7. HEK 293 cells were transfected with pRLTK control plasmid; a luciferase reporter plasmid containing the IRF-7-responsive IFNA4 promoter; and either a control plasmid or a plasmid encoding wt (IRF-7 WT), a series of serine-to-alanine (A and B) mutants of IRF-7, or a series of serine-to-aspartic acid (C and D) mutants of IRF-7, in the absence (C) or the presence of either IKKε (A) or TBK1 (B and D) as indicated. The point mutation of the IRF-7 plasmid is indicated under each bar. Luciferase activity was analyzed 24 h posttransfection as fold activation relative to the basal level of reporter gene in the presence of control vector (after normalization with cotransfected *Renilla* relative light units). Values represent the averages of three independent experiments performed in duplicate, with variability shown by error bars.

pression of wt and point-mutated IRF-7 forms alone resulted in a relatively modest 10- to 30-fold stimulation of IFNA4 promoter activity (data not shown). On the other hand, coexpression of wt IRF-7 together with IKKε (Fig. 9A) or TBK1 (Fig. 9B) enhanced IFNA4 reporter activity up to 2,000-fold. IRF-7 proteins with mutations in two distinct clusters—S471/472A and S483/487A—were unable to respond to IKKε (Fig. 9A) or TBK1 (Fig. 9B) activation; an IRF-7 form that was mutated at S477/479A was also severely reduced, implicating these residues as important sites for IRF-7 activation. Interestingly, replacement of four serines at aa 475 to 479 with the phosphomimetic Asp generated a form of IRF-7 that transactivated IFNA4 ~800-fold in the absence of stimulation (Fig. 9C). Other Asp substitutions within the aa 475 to 479 cluster also generated active forms of IRF-7 (Fig. 9C, D475/476, D477/479, D479, and D477), but these were not as active as the D475-479 construct. Cotransfection with TBK1 activated wt IRF-7 as well as Asp mutants to very high levels (2,000- to 6,000-fold stimulation) (Fig. 9D). Interestingly, mutation of Ser471 and Ser472 to Asp generated an inactive form of IRF-7 that was unresponsive to virus infection (25) or TBK1 activation (Fig. 9C and D). By analogy with IRF-3 Ser residues at 385 and 386 (19, 58), mutation of these Ser residues within the SSL motif of IRF-7 at positions 471 to 473 resulted in a protein that was transcriptionally inert. In contrast, Ser residues at positions 477 and 479 of IRF-7, like the Ser residues at 396 and 398 in IRF-3, produced constitutively active IRF proteins when mutated to Asp and a dramatic reduction in their inducibility by either TBK1 or IKKε when replaced with Ala residues (Fig. 9A and B). Mutation of the Ser residues at positions 483 and 487 to Ala totally eliminated both virus and IKKε and TBK1 activation (Fig. 9A and B); however, mutation of these two residues to Asp resulted in a protein that had no constitutive activity (Fig. 9C) but was still fully inducible by TBK1 (Fig. 9D) or virus infection (data not shown). In total, both TBK1 and IKKε share closely related specificities for the C-terminal serine residues of both IRF-3 and IRF-7 that have an impact on the inducibility of IRF-7 in coexpression studies.

DISCUSSION

The initial demonstration that the virus-activated kinase activity responsible for IRF-3 and IRF-7 C-terminal phosphorylation is TBK1 and that its inducible counterpart is IKKε (8, 49) provides an important link between TLR signaling and the IRF transcription factors (7, 9). Although both LPS and dsRNA induce IRF-3 activation in a TLR-dependent manner (7), virus-induced activation of IRF-3 is not abolished in the absence of TLR3 or the TIR adaptor molecule TRIF. Clearly, dsRNA-induced TLR3 signaling into IRF-3 and IRF-7 activation via TBK1 and IKKε represents a fundamental mechanism for IFN-α/β production in mammalian cells, although TLR3 engagement by dsRNA (1) is not the sole trigger for TBK1-IKKε activation in the context of de novo virus infection. Since VSV infection induced IRF-3 phosphorylation in a TRIF- and TLR3-independent manner, a viral structural component could be involved in TBK1 activation. Both measles virus and Sendai virus nucleocapsid proteins were shown previously to induce IRF-3 phosphorylation (47, 54), and with the present study, we demonstrate that RNP complexes isolated from whole VSV virions activated TBK1 kinase and induced IRF-3 phosphorylation with kinetics similar to those observed with VSV infection. Furthermore, the delayed kinetics of TBK1 induction by RNP compared to the rapid kinetics with dsRNA (3 h versus 30 min, respectively) suggested distinct mechanisms of detection, and in this regard, RNP appears to represent a TLR3-independent, intracellular mimic of virus infection. The recent demonstration that TLR7 recognizes single-stranded RNA viruses such as VSV and influenza virus is consistent with the present results (6, 14, 28) and suggests that RNP may deliver single-stranded RNA to the endosome compartment where it is sensed by TLR7 and/or that an additional TLR-like mechanism recognizes a protein component of RNP. Furthermore entry of enveloped virus particles from diverse virus families is sufficient to elicit a similar innate IRF-3-dependent response (5).

Direct in vitro phosphorylation of IRF-3 and IRF-7 with purified recombinant IKKε and TBK1 demonstrated that the two kinases exhibit identical specificity in vitro for carboxyl-terminal Ser/Thr sites. Our results are in agreement with those of McWhirter et al. (30) and demonstrate that mutation of the five cluster II residues to alanine abolished the majority of TBK1- or IKKε-directed phosphorylation; the residual kinase activity was completely abolished with further mutation of the cluster I residues at S385/386. Thus, TBK1 and IKKε primarily target the cluster II S/T residues. Furthermore, mutation of Ser402 abolished most of the direct phosphorylation; this result is consistent with the consensus recognition motif of TBK1 and IKKε, previously established in vitro with the SXXXS motif of IκBα (36, 50). However, identification of S402 as the target site for TBK1 and IKKε, together with the identification of Ser396 as the essential residue for IRF-3 activation (47), suggests that phosphorylation at S402 by TBK1 and IKKε may represent the initial step of a multistep process (26, 37) involving IKKε and TBK1 and/or potentially another, as-yet-unidentified kinase.

Phosphorylation of the IRF-7 carboxyl terminus by the TBK1 and IKKε directly targets two Ser residues, S477 and S479. Mutation of these residues to Ala abolished TBK1 and IKKε phosphorylation of the IRF-7 carboxyl terminus. These results are consistent with the functional analysis of IRF-7: an S477/479D phosphomimetic mutation enhanced the IRF-7 transactivation of the IFNA4 promoter, whereas Ala substitution abolished the IRF-7 transactivation in response to VSV infection. The S479 residue also lies within an SXXXS consensus motif; however, in vitro kinase assays indicated that an S479A substitution only partially diminished direct TBK1 and IKKε phosphorylation. The diversity of substrate recognition by the TBK1 and IKKε kinases for the carboxy terminus of IRF-7 suggests that there is still much to be learned about the enzymatic specificity of IKKε and TBK1.

The differential expression of TBK1 and IKKε may reflect distinct, nonredundant roles in the activation of IFN signaling. TBK1 is constitutively and ubiquitously expressed (3) and correlates with the expression of IRF-3 (2, 24, 27), while IKKε expression is inducible in nonhematopoietic cells in response to a variety of stimuli including LPS and phorbol ester (21, 36, 50). The expression pattern of IKKε in fact is reminiscent of that of IRF-7, which is also regulated at the transcriptional level (29, 41). In an effort to discern the functional differences between TBK1 and IKKε, the effects of VSV, dsRNA, and RNP treatment were compared in $TBK^{-/-}$ MEFs, and a dramatic decrease in IRF-3 phosphorylation was observed in cells lacking TBK1. However, in contrast to the results of McWhirter et al. (30) C-terminal IRF-3 phosphorylation and transcriptional activity were not completely abolished; rather a delayed kinetics of induction was observed that correlated with upregulation of IKKε expression. The induction of IKKε kinase activity may in fact partially compensate for the TBK1 defect.

Identification of the specific virus-responsive phosphoacceptor sites within the carboxyl-terminal signal-responsive regions of IRF-3 and IRF-7 has been the focus of significant effort. Characterization of these sites is important, with implications for the development of efficient analytical reagents to monitor IRF-3 and IRF-7 activation in vivo. Mutagenesis of the IRF-3 carboxyl-terminal domain has been performed previously to determine which residues are targeted for phosphorylation during virus infection. Mutation of the cluster I Ser385/386 to Ala abolished IRF-3 transcriptional activity in response to virus infection (58); however, mutation of S385/386 to the phosphomimetic Asp, which should mimic the effect of constitutive phosphorylation, also eliminated IRF-3 activity (26). These results can be interpreted as the S385/386 cluster being important as a recognition domain, as opposed to a direct phosphoacceptor target, or alternatively the results may also indicate that phosphomimetic substitutions do not always yield a functional protein.

Mutational analyses of the cluster II residues indicated that five S/T residues within this region (S396, S398, S402, T404, and S405) are important for virus-inducible IRF-3 activation (24, 26). Alanine substitution for the five S/T cluster II residues in IRF-3(5A) dramatically reduced IRF-3 activation in response to virus infection (26). Significantly, mutation of the five cluster II residues to the phosphomimetic Asp generated a constitutively active IRF-3 that efficiently induced IRF-3-dependent promoters (24, 26) and stimulated cellular apoptosis in the absence of virus infection (15).

The three-dimensional crystal structure of the IRF-3 carbox-

yl-terminal domain has recently been reported (37, 52). Qin et al. interpreted the structure in light of a unique autoinhibitory mechanism in which amino- and carboxy-terminal α-helical structures flanking a β-sandwich IAD core interact to form a condensed hydrophobic structure (26, 37). The interaction buries several key residues that are involved in dimerization of the active protein and therefore are required for nuclear accumulation, DNA binding, and transactivation. Virus-inducible, carboxyl-terminal phosphorylation abolishes autoinhibitory interactions by introducing charge repulsions that unmask the active site and realign the DNA binding domain to form the transcriptionally active protein (37). Significantly, Qin et al. maintain that multiple serine/threonine phosphorylation events within the cluster I and cluster II residues are required for relief of latent autoinhibition.

Takahasi et al. undertook an X-ray crystallography approach to study the structure of the IRF-3 carboxy terminus, coupled with evaluation of the dimerization capacity of IRF-3 (52). These experiments also assert that phosphorylation of the carboxy terminus directly precipitates IRF-3 dimerization and generates an acidic pocket responsible for p300/CBP association. This group maintains that the cluster I residues—particularly the S386 residue—are the initial target for virus-inducible, as well as IKKε- and TBK1-mediated, IRF-3 phosphorylation during IRF-3 activation, because the cluster I residues are the most accessible amino acids (52). In contrast, Qin et al. emphasize a sequential mechanism of IRF-3 carboxy-terminal phosphorylation. Although the cluster I residues are exposed in latent IRF-3, residues within both serine clusters, I and II, are required to serve as kinase recognition and/or direct phosphoacceptor sites, and sequential phosphorylation of both clusters is necessary to elicit complete unfolding and activation of IRF-3 (37). Interestingly, both groups observed that the carboxyl terminus of IRF-3 exhibits a similarity to the Mad homology 2 (MH2) domain of the Smad family of transcription factors, with respect to structural integrity and surface electrostatic potential. This similarity suggests a common molecular mechanism of action among a superfamily of signaling mediators and further implies that IRF and Smad transcription factors may have a common evolutionary origin with the potential for regulatory cross talk (37, 52).

ACKNOWLEDGMENTS

We thank Ganes Sen (Cleveland) and John Bell (Ottawa) for reagents and members of the Molecular Oncology Group, Lady Davis Institute, McGill University, for helpful discussions.

This research was supported by grants from the Canadian Institutes of Health Research, the National Cancer Institute with funds from the Canadian Cancer Society and CANVAC, and the Canadian Vaccine and Immunotherapeutics Initiative. S.S. was supported by a CIHR studentship, B.R.T. was supported by an NSERC Studentship, N.G. was supported by an FRSQ Post-doctoral Fellowship, R.L. was supported by an FRSQ Chercheur Boursier, and J.H. was supported by a CIHR Senior Investigator award.

REFERENCES

1. **Alexopoulou, L., A. C. Holt, R. Medzhitov, and R. A. Flavell.** 2001. Recognition of double-stranded RNA and activation of NF-κB by Toll-like receptor 3. Nature **413:**732–738.
2. **Au, W. C., P. A. Moore, W. Lowther, Y. T. Juang, and P. M. Pitha.** 1995. Identification of a member of the interferon regulatory factor family that binds to the interferon-stimulated response element and activates expression of interferon-induced genes. Proc. Natl. Acad. Sci. USA **92:**11657–11661.
3. **Bonnard, M., C. Mirtsos, S. Suzuki, K. Graham, J. Huang, M. Ng, A. Itie, A. Wakeham, A. Shahinian, W. J. Henzel, A. J. Elia, W. Shillinglaw, T. W. Mak, Z. Cao, and W. C. Yeh.** 2000. Deficiency of T2K leads to apoptotic liver degeneration and impaired NF-κB-dependent gene transcription. EMBO J. **19:**4976–4985.
4. **Chu, W. M., D. Ostertag, Z. W. Li, L. Chang, Y. Chen, Y. Hu, B. Williams, J. Perrault, and M. Karin.** 1999. JNK2 and IKKβ are required for activating the innate response to viral infection. Immunity **11:**721–731.
5. **Collins, S. E., R. S. Noyce, and K. L. Mossman.** 2004. Innate cellular response to virus particle entry requires IRF3 but not virus replication. J. Virol. **78:**1706–1717.
6. **Diebold, S. S., T. Kaisho, H. Hemmi, S. Akira, and E. S. C. Reis.** 2004. Innate antiviral responses by means of TLR7-mediated recognition of single-stranded RNA. Science **303:**1529–1531.
7. **Doyle, S., S. Vaidya, R. O'Connell, H. Dadgostar, P. Dempsey, T. Wu, G. Rao, R. Sun, M. Haberland, R. Modlin, and G. Cheng.** 2002. IRF3 mediates a TLR3/TLR4-specific antiviral gene program. Immunity **17:**251–263.
8. **Fitzgerald, K. A., S. M. McWhirter, K. L. Faia, D. C. Rowe, E. Latz, D. T. Golenbock, A. J. Coyle, S. M. Liao, and T. Maniatis.** 2003. IKKε and TBK1 are essential components of the IRF3 signaling pathway. Nat. Immunol. **4:**491–496.
9. **Fitzgerald, K. A., D. C. Rowe, B. J. Barnes, D. R. Caffrey, A. Visintin, E. Latz, B. Monks, P. M. Pitha, and D. T. Golenbock.** 2003. LPS-TLR4 signaling to IRF-3/7 and NF-κB involves the Toll adapters TRAM and TRIF. J. Exp. Med. **198:**1043–1055.
10. **Gale, M., S. L. Tan, and M. G. Katze.** 2000. Translational control of viral gene expression in eukaryotes. Microbiol. Mol. Biol. Rev. **64:**239–280.
11. **Genin, P., M. Algarte, P. Roof, R. Lin, and J. Hiscott.** 2000. Regulation of RANTES chemokine gene expression requires cooperativity between NF-κB and IFN-regulatory factor transcription factors. J. Immunol. **164:**5352–5361.
12. **Grandvaux, N., M. J. Servant, B. tenOever, G. C. Sen, S. Balachandran, G. N. Barber, R. Lin, and J. Hiscott.** 2002. Transcriptional profiling of interferon regulatory factor 3 target genes: direct involvement in the regulation of interferon-stimulated genes. J. Virol. **76:**5532–5539.
13. **Grandvaux, N., B. R. tenOever, M. J. Servant, and J. Hiscott.** 2002. The interferon antiviral response: from viral invasion to evasion. Curr. Opin. Infect. Dis. **15:**259–267.
14. **Heil, F., H. Hemmi, H. Hochrein, F. Ampenberger, C. Kirschning, S. Akira, G. Lipford, H. Wagner, and S. Bauer.** 2004. Species-specific recognition of single-stranded RNA via toll-like receptor 7 and 8. Science **303:**1526–1529.
15. **Heylbroeck, C., S. Balachandran, M. Servant, C. DeLuca, G. Barber, R. Lin, and J. Hiscott.** 2000. The IRF-3 transcription factor mediates Sendai virus-induced apoptosis. J. Virol. **74:**3781–3792.
16. **Hoebe, K., X. Du, P. Georgel, E. Janssen, K. Tabeta, S. O. Kim, J. Goode, P. Lin, N. Mann, S. Mudd, K. Crozat, S. Sovath, J. Han, and B. Beutler.** 2003. Identification of Lps2 as a key transducer of MyD88-independent TIR signalling. Nature **424:**743–748.
17. **Huynh, Q. K., N. Kishore, S. Mathialagan, A. M. Donnelly, and C. S. Tripp.** 2002. Kinetic mechanisms of IκB-related kinases (IKK) inducible IKK and TBK-1 differ from IKK-1/IKK-2 heterodimer. J. Biol. Chem. **277:**12550–12558.
18. **Iordanov, M. S., J. M. Paranjape, A. Zhou, J. Wong, B. R. Williams, E. F. Meurs, R. H. Silverman, and B. E. Magun.** 2000. Activation of p38 mitogen-activated protein kinase and c-Jun NH_2-terminal kinase by double-stranded RNA and encephalomyocarditis virus: involvement of RNase L, protein kinase R, and alternative pathways. Mol. Cell. Biol. **20:**617–627.
19. **Juang, Y., W. Lowther, M. Kellum, W. C. Au, R. Lin, J. Hiscott, and P. M. Pitha.** 1998. Primary activation of interferon A and interferon B gene transcription by interferon regulatory factor 3. Proc. Natl. Acad. Sci. USA **95:**9837–9842.
20. **Kishore, N., Q. K. Huynh, S. Mathialagan, T. Hall, S. Rouw, D. Creely, G. Lange, J. Caroll, B. Reitz, A. Donnelly, H. Boddupalli, R. G. Combs, K. Kretzmer, and C. S. Tripp.** 2002. IKK-i and TBK-1 are enzymatically distinct from the homologous enzyme IKK-2: comparative analysis of recombinant human IKK-i, TBK-1, and IKK-2. J. Biol. Chem. **277:**13840–13847.
21. **Kravchenko, V. V., J. C. Mathison, K. Schwamborn, F. Mercurio, and R. J. Ulevitch.** 2003. IKKi/IKKε plays a key role in integrating signals induced by pro-inflammatory stimuli. J. Biol. Chem. **278:**26612–26619.
22. **Lin, R., P. Genin, Y. Mamane, and J. Hiscott.** 2000. Selective DNA binding and association with the CREB binding protein coactivator contribute to differential activation of alpha/beta interferon genes by interferon regulatory factors 3 and 7. Mol. Cell. Biol. **20:**6342–6353.
23. **Lin, R., C. Heylbroeck, P. Genin, P. Pitha, and J. Hiscott.** 1999. Essential role of IRF-3 in direct activation of RANTES gene transcription. Mol. Cell. Biol. **19:**959–966.
24. **Lin, R., C. Heylbroeck, P. M. Pitha, and J. Hiscott.** 1998. Virus-dependent phosphorylation of the IRF-3 transcription factor regulates nuclear translocation, transactivation potential, and proteasome-mediated degradation. Mol. Cell. Biol. **18:**2986–2996.
25. **Lin, R., Y. Mamane, and J. Hiscott.** 2000. Multiple regulatory domains control IRF-7 activity in response to virus infection. J. Biol. Chem. **275:**34320–34327.
26. **Lin, R., Y. Mamane, and J. Hiscott.** 1999. Structural and functional analysis

of interferon regulatory factor 3: localization of the transactivation and autoinhibitory domains. Mol. Cell. Biol. **19:**2465–2474.
27. **Lowther, W. J., P. A. Moore, K. C. Carter, and P. M. Pitha.** 1999. Cloning and functional analysis of the human IRF-3 promoter. DNA Cell Biol. **18:**685–692.
28. **Lund, J. M., L. Alexopoulou, A. Sato, M. Karow, N. C. Adams, N. W. Gale, A. Iwasaki, and R. A. Flavell.** 2004. Recognition of single-stranded RNA viruses by Toll-like receptor 7. Proc. Natl. Acad. Sci. USA **101:**5598–5603.
29. **Marie, I., J. E. Durbin, and D. E. Levy.** 1998. Differential viral induction of distinct interferon-alpha genes by positive feedback through interferon regulatory factor-7. EMBO J. **17:**6660–6669.
30. **McWhirter, S. M., K. A. Fitzgerald, J. Rosains, D. C. Rowe, D. T. Golenbock, and T. Maniatis.** 2004. IFN-regulatory factor 3-dependent gene expression is defective in Tbk1-deficient mouse embryonic fibroblasts. Proc. Natl. Acad. Sci. USA **101:**233–238.
31. **Medzhitov, R., and C. A. Janeway, Jr.** 2002. Decoding the patterns of self and nonself by the innate immune system. Science **296:**298–300.
32. **Mori, M., M. Yoneyama, T. Ito, K. Takahashi, F. Inagaki, and T. Fujita.** 2004. Identification of Ser 386 of interferon regulatory factor 3 as critical targets for inducible phosphorylation that determines activation. J. Biol. Chem. **279:**9698–9702.
33. **Moyer, S. A., S. Smallwood-Kentro, A. Haddad, and L. Prevec.** 1991. Assembly and transcription of synthetic vesicular stomatitis virus nucleocapsids. J. Virol. **65:**2170–2178.
34. **Oshiumi, H., M. Matsumoto, K. Funami, T. Akazawa, and T. Seya.** 2003. TICAM-1, an adaptor molecule that participates in Toll-like receptor 3-mediated interferon-beta induction. Nat. Immunol. **4:**161–167.
35. **Patterson, J. L., and R. Fernandez-Larsson.** 1990. Molecular mechanisms of action of ribavirin. Rev. Infect. Dis. **12:**1139–1146.
36. **Peters, R. T., S. M. Liao, and T. Maniatis.** 2000. IKKε is part of a novel PMA-inducible IκB kinase complex. Mol. Cell **5:**513–522.
37. **Qin, B. Y., C. Liu, S. S. Lam, H. Srinath, R. Delston, J. J. Correia, R. Derynck, and K. Lin.** 2003. Crystal structure of IRF-3 reveals mechanism of autoinhibition and virus-induced phosphoactivation. Nat. Struct. Biol. **10:** 913–921.
38. **Rassa, J. C., and S. R. Ross.** 2003. Viruses and Toll-like receptors. Microbes Infect. **5:**961–968.
39. **Sabroe, I., R. C. Read, M. K. Whyte, D. H. Dockrell, S. N. Vogel, and S. K. Dower.** 2003. Toll-like receptors in health and disease: complex questions remain. J. Immunol. **171:**1630–1635.
40. **Samuel, C. E.** 2001. Antiviral actions of interferons. Clin. Microbiol. Rev. **14:**778–809.
41. **Sato, M., N. Hata, M. Asagiri, T. Nakaya, T. Taniguchi, and N. Tanaka.** 1998. Positive feedback regulation of type I IFN genes by the IFN-inducible transcription factor IRF-7. FEBS Lett. **441:**106–110.
42. **Sato, M., H. Suemori, N. Hata, M. Asagiri, K. Ogasawara, K. Nakao, T. Nakaya, M. Katsuki, S. Noguchi, N. Tanaka, and T. Taniguchi.** 2000. Distinct and essential roles of transcription factors IRF-3 and IRF-7 in response to viruses for IFN-alpha/beta gene induction. Immunity **13:**539–548.
43. **Sato, M., N. Tanaka, N. Hata, E. Oda, and T. Taniguchi.** 1998. Involvement of the IRF family transcription factor IRF-3 in virus-induced activation of the IFN-beta gene. FEBS Lett. **425:**112–116.
44. **Sato, S., M. Sugiyama, M. Yamamoto, Y. Watanabe, T. Kawai, K. Takeda, and S. Akira.** 2003. Toll/IL-1 receptor domain-containing adaptor inducing IFN-beta (TRIF) associates with TNF receptor-associated factor 6 and TANK-binding kinase 1, and activates two distinct transcription factors, NF-κB and IFN-regulatory factor-3, in the Toll-like receptor signaling. J. Immunol. **171:**4304–4310.
45. **Sen, G. C.** 2001. Viruses and interferons. Annu. Rev. Microbiol. **55:**255–281.
46. **Servant, M. J., N. Grandvaux, and J. Hiscott.** 2002. Multiple signaling pathways leading to the activation of interferon regulatory factor 3. Biochem. Pharmacol. **64:**985–992.
47. **Servant, M. J., N. Grandvaux, B. R. TenOever, D. Duguay, R. Lin, and J. Hiscott.** 2003. Identification of the minimal phosphoacceptor site required for in vivo activation of IRF-3 in response to virus and dsRNA. J. Biol. Chem. **278:**9441–9447.
48. **Servant, M. J., B. ten Oever, C. LePage, L. Conti, S. Gessani, I. Julkunen, R. Lin, and J. Hiscott.** 2001. Identification of distinct signaling pathways leading to the phosphorylation of interferon regulatory factor 3. J. Biol. Chem. **276:**355–363.
49. **Sharma, S., B. R. tenOever, N. Grandvaux, G. P. Zhou, R. Lin, and J. Hiscott.** 2003. Triggering the interferon antiviral response through an IKK-related pathway. Science **300:**1148–1151.
50. **Shimada, T., T. Kawai, K. Takeda, M. Matsumoto, J. Inoue, Y. Tatsumi, A. Kanamaru, and S. Akira.** 1999. IKK-i, a novel lipopolysaccharide-inducible kinase that is related to IκB kinases. Int. Immunol. **11:**1357–1362.
51. **Smith, E. J., I. Marie, A. Prakash, A. Garcia-Sastre, and D. E. Levy.** 2001. IRF3 and IRF7 phosphorylation in virus-infected cells does not require double-stranded RNA-dependent protein kinase R or IκB kinase but is blocked by vaccinia virus E3L protein. J. Biol. Chem. **276:**8951–8957.
52. **Takahasi, K., N. N. Suzuki, M. Horiuchi, M. Mori, W. Suhara, Y. Okabe, Y. Fukuhara, H. Terasawa, S. Akira, T. Fujita, and F. Inagaki.** 2003. X-ray crystal structure of IRF-3 and its functional implications. Nat. Struct. Biol. **10:**922–927.
53. **Takeda, K., and S. Akira.** 2004. TLR signaling pathways. Semin. Immunol. **16:**3–9.
54. **tenOever, B. R., M. J. Servant, N. Grandvaux, R. Lin, and J. Hiscott.** 2002. Recognition of the measles viral nucleocapsid as a mechanism of IRF-3 activation. J. Virol. **76:**3659–3669.
55. **Weaver, B. K., O. Ando, K. P. Kumar, and N. C. Reich.** 2001. Apoptosis is promoted by the dsRNA-activated factor (DRAF1) during viral infection independent of the action of interferon or p53. FASEB J. **15:**501–515.
56. **Yamamoto, M., S. Sato, H. Hemmi, K. Hoshino, T. Kaisho, H. Sanjo, O. Takeuchi, M. Sugiyama, M. Okabe, K. Takeda, and S. Akira.** 2003. Role of adaptor TRIF in the MyD88-independent Toll-like receptor signaling pathway. Science **301:**640–643.
57. **Yamamoto, M., S. Sato, K. Mori, K. Hoshino, O. Takeuchi, K. Takeda, and S. Akira.** 2002. Cutting edge: a novel Toll/IL-1 receptor domain-containing adapter that preferentially activates the IFN-beta promoter in the Toll-like receptor signaling. J. Immunol. **169:**6668–6672.
58. **Yoneyama, M., W. Suhara, Y. Fukuhara, M. Fukada, E. Nishida, and T. Fujita.** 1998. Direct triggering of the type I interferon system by virus infection: activation of a transcription factor complex containing IRF-3 and CBP/p300. EMBO J. **17:**1087–1095.